Dynamic Centrifuge Test of an Embankment on Liquefiable Soil Reinforced with Soil-Cement Walls

Ali Khosravi, Mohammad Khosravi, Ross W. Boulanger, Daniel W. Wilson, Amber Pulido
Department of Civil and Environmental Engineering, University of California, Davis, CA, USA, akhosravi@ucdavis.edu

ABSTRACT
This paper describes the model construction procedure and presents example results and preliminary observations for a centrifuge test of an embankment on a liquefiable foundation layer treated with soil-cement walls and subjected to seismic loads. The centrifuge experiment was carried out on the 9-m radius centrifuge at the Center for Geotechnical Modeling at UC Davis. The model corresponded to, in prototype units, a 28-m tall embankment of coarse medium dense Monterey sand (relative density, $D_r \approx 85\%$) underlain by a 9-m thick saturated loose Ottawa sand layer with D_r of about 42%. Soil-cement walls were constructed through the loose sand layer over a 30-m long section near the toe of the embankment and covered with a 7.5-m tall berm. The soil-cement had an average unconfined compressive strength of 2.0 MPa and the walls had an area replacement ratio of 24% over the width of the embankment. The model was shaken with a series of scaled earthquakes having peak horizontal base accelerations ranging from 0.05g to 0.54 g. This paper describes the model construction procedure (e.g. sand pluviation, soil-cement wall construction, instrumentation), and presents some preliminary results and observations of the performance of the soil, embankment, and soil-cement walls.

1 INTRODUCTION

Mitigation of earthquake damage potential at soft or liquefiable soil sites remains a challenge in earthquake engineering. Earthquake damage potential at soft or liquefiable soil sites can be reduced, for example, by reinforcing the soil to support overlying structures, increasing the composite shear strength of the profile, reducing the seismic stresses and strains in the soils (e.g., by using stone columns, cement soil mixing, jet grouting), or by removing and replacing the weak soils with competent soils (Mitchell 2008).

Soil-cement grid and wall systems constructed by the deep mixing method (DMM), jet grouting or other methods have been used in practice to reduce earthquake damage potential in embankment dams. These types of reinforcements can act as shear reinforcement to reduce shear stresses in the enclosed soils and thus prevent liquefaction triggering, and they can provide increased composite strength to resist deformations even if the enclosed soils liquefy during strong shaking. Several previous studies on soil-cement reinforcement have illustrated the beneficial effects of soil-cement ground reinforcement on reducing settlements or other ground failure modes in soft or liquefiable soils (e.g. Babasaki et al. 1991, Kitazume et al. 1996, Rayamajhi et al. 2015a,b, Khosravi et al. 2015a,b, Tamura et al. 2016, Khosravi et al. 2016a). Few studies in the literature, however, have documented in detail the effect of soil-cement ground reinforcement on seismic response of embankments founded on such an improved site (e.g. Adalier et al., 1998). Common concerns regarding the use of soil-cement walls for liquefaction remediation beneath embankments are the potential for cracking and brittle failure, and the lack of experimental or case history data to confidently validate 2D or 3D numerical analysis methods.

This paper describes an experimental study which was conducted to study: 1) the seismic response of an embankment built upon a loose liquefiable sand reinforced with soil-cement walls, and 2) the shear response and performance of the soil-cement wall reinforcements under loading strong enough to extensively damage the walls. The test was performed at a centrifugal acceleration of 65 g on the 9-m radius centrifuge at the Center for Geotechnical Modeling at the University of California at Davis. The model corresponded to, in prototype units, a 28-m tall embankment of coarse medium dense Monterey sand (relative density, $D_r \approx 80\%$) underlain by a 9-m thick saturated loose Ottawa sand layer with D_r of about 42%. Soil-cement walls were constructed through the loose sand layer over a 30-m long section near the toe of the embankment and covered with a 7.5-m tall berm. The soil-cement had an average unconfined compressive strength of 2.0 MPa and the walls had an area replacement ratio of 24% over the width of the embankment. The model was shaken three times with a scaled seismic motion having peak horizontal base accelerations ranging from 0.05g to 0.55 g. The following sections describe the centrifuge test, the model construction procedures, representative recorded responses, and initial observations regarding performance of the soil-cement wall system.

2 CENTRIFUGE TEST PROGRAM

A centrifuge test was performed of an embankment model on the 9-m radius centrifuge at the University of California at Davis and the data archived for general distribution

(Khosravi et al. 2016b). The test was performed at a centrifugal acceleration of 65g. The recorded data and model dimensions were converted into prototype units according to the scaling laws as described by Kutter (1995). All data are presented in prototype units unless otherwise specified.

The test model was prepared in a "flexible shear beam container" (Wilson et al. 1997). The inner dimensions of the container in model scale were 1700 mm long (110 m in prototype), 700mm wide (46 m in prototype) and 700 mm high (46 m in prototype). The shear beam container consists of 4 aluminum shear rings stacked together and separated by sheets of 12 mm-thick Neoprene rubber.

The model consisted of an embankment built upon the loose liquefiable sand reinforced with soil-cement walls as shown in Figure 1. A relatively thick layer (9 m) of Ottawa sand (D_{50} = 0.14 mm) was used as liquefiable soil layer and coarse Monterey sand (D_{50} = 0.40 mm) was used as the embankment. The selected properties of Ottawa and coarse Monterey sands are shown in Table 1.

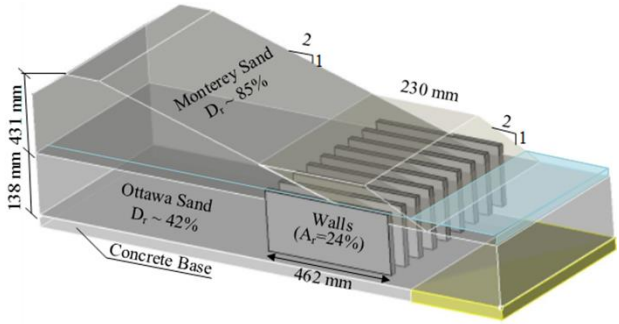

Figure 1. 3D Model Configuration; Dimensions in Model Units (mm)

Table 1- Selected parameters for sand used in the test

Soil Type	Soil Classi-fication	Grain Size (mm)		Specific Gravity	Void Ratio	
		D_{50}	D_{10}	G_s	e_{max}	e_{min}
Monterey Sand	SP	0.95	0.98	2.64	0.84	0.54
Ottawa Sand-F65	SP	0.2	0.14	2.66	0.84	0.49

2.1 Soil-Cement Wall Construction

A series of soil-cement walls were fabricated from a mixture of soil (Ottawa sand F65), cement, and water with a weight proportion presented in Table 2. The pre-casting procedure for the soil-cement walls is presented in Figure 2. After carefully mixing the cement, sand, and water to ensure homogeneity, the slurry was shaped in a mold to form rectangular panels having model dimensions of 462.0 mm × 205.0 mm and thickness of approximately 22.0 mm as shown in Figure 2a. The inside surface of the molds was covered by 0.012" thick Wear-Resistant Slippery UHMW tape to facilitate removing the walls from inside the molds after curing. After casting, the walls were cured at room temperature for about 14 days. The soil-cement had an unconfined compressive strength of 2.0 MPa after 14 days (curing time), as measured using test cylinders cast in parallel to the walls.

Table 2. Soil Cement Mixtures

No.	Mixture Ratio (by weight)		
	Cement	Sand	Water
Wall	1.0	10.5	2.75
Base	1.0	5.0	1.63

In order to monitor the performance of the soil-cement walls during and after shaking, an innovative type of crack detector (CD) was cast into select walls. The crack detector is simply a 2-mm pencil lead connecting to two wires at the ends. Pencil lead has a very small resistance (1-2 Ω) initially that significantly increases when cracking occurs along the crack detector. More details about the crack detector can be found in Tamura et al. (2015). The crack detectors (CD) were embedded in the soil-cement walls at the target locations before it cured (Figure 2b).

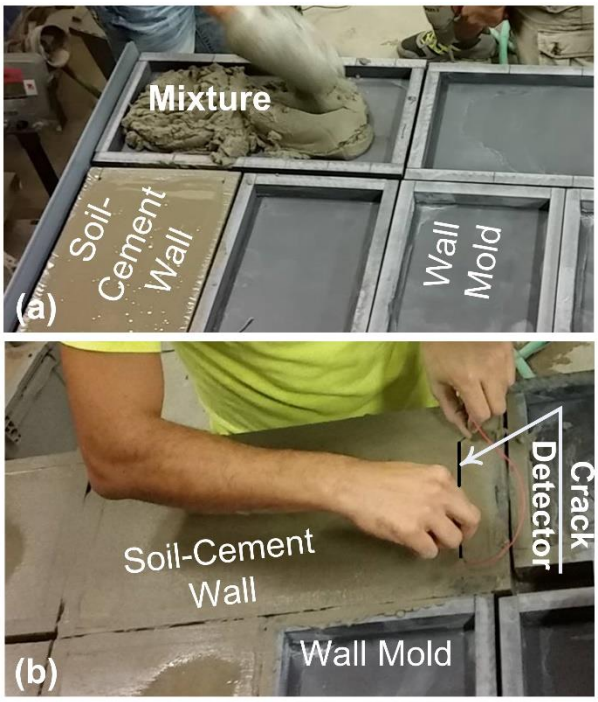

Figure 2. Soil-cement wall construction procedure: a) pouring the soil-cement mixture in the molds, b) placing crack detector in the walls

2.2 Model Construction

The model construction procedure and final model are shown in Figs. 3 and 4. After curing, the prefabricated soil cement walls were removed from the molds and placed inside a series of tooled grooves in the concrete base with a center-to-center spacing of 70 mm (model scale). To attach the soil-cement walls to the concrete base, the grooves were first filled up partially with cement slurry, then the soil-cement walls were pushed in the grooves as shown in Figure 3a.

After placing the pre-fabricated walls, the lower loose sand layer for the model was constructed in multiple lifts using dry pluviation. The pluviation was carried out to achieve a D_r of about 42% for Ottawa sand as the loose liquefiable layer and a D_r of about 85% for coarse Monterey sand as the embankment. A coarse Aquarium sand of 1 cm (model dimensions) thick was also placed in the embankment (about 2 cm above the loose sand layer) to prevent capillary rise of viscous fluid in the embankment at 1g. The pluviation process was interrupted at pre-defined elevations for the placement of the sensors.

After completion of dry pluviation of the loose Ottawa sand layer, 3 cm (model scale) of the embankment and the Aquarium sand, the model was placed on the centrifuge arm and then saturated. For saturation, an aluminum lid was placed over the container, then the model was flushed with three cycles of carbon dioxide gas with the application of a vacuum after each cycle of carbon dioxide flushing to ensure there is no air trapped in the sample and the concrete base. The introduction of pore fluid was carried out under vacuum with a de-aired mixture of methyl-cellulose and de-ionized water having a viscosity approximately 20 times higher than water. The saturation progressed from bottom of the container to top of the aquarium sand ensuring full saturation of the lower sand layer. It took about 5 days for the complete saturation of the model. The final water level was brought to 1 cm (model scale) above the top of aquarium sand layer before releasing the vacuum to ensure full saturation of the soil foundation. The water over the aquarium sand layer was later removed before pluviation of the embankment. The water level was kept underneath the aquarium sand layer during embankment construction.

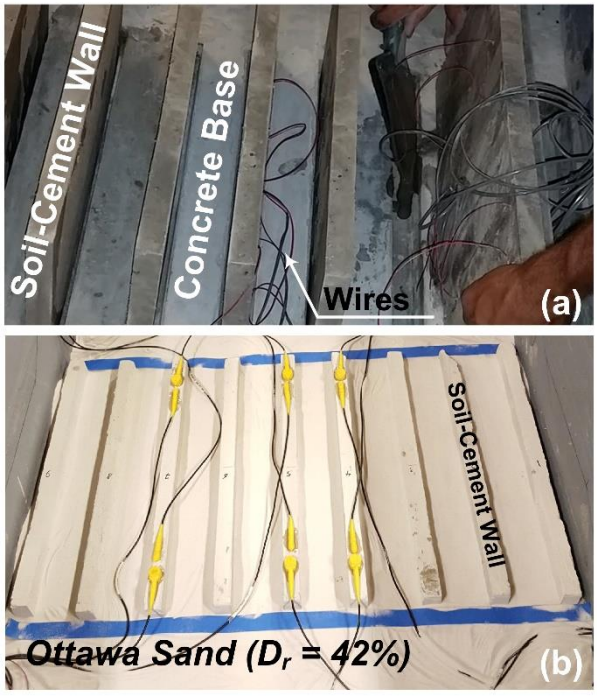

Figure 3. Model construction procedure: a) soil-cement wall attachment to the concrete base, b) soil-cement walls after construction and sand Pluviation.

After completion of the saturation of the loose sand layer, the container lid was removed and the embankment was completed by dry pluviation (Figure 4). The remaining instrumentation (e.g., accelerometers in the embankment and linear potentiometers) was then placed on the arm.

The model was instrumented with three types of transducers commonly used in centrifuge tests including vertical and horizontal accelerometers (ACC), pore pressure transducers (PPTs), and linear potentiometers (LPs). The locations of select accelerometers, pore pressure transducers, and linear potentiometers are shown in Figure 5. A total of 63 ACCs, 22 PPTs, 8, and 17 CDs were included in the centrifuge model.

Figure 4. Embankment model after completion

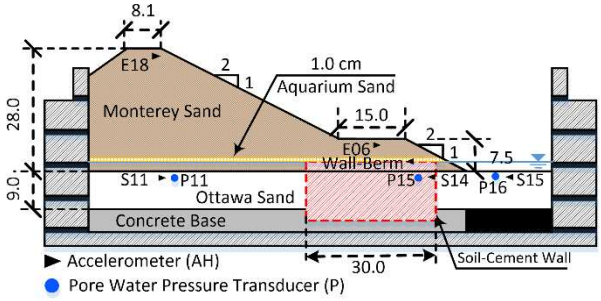

Figure 5. Cross-section of the model showing locations of accelerometers and pore pressure transducers; dimensions in prototype units (m)

To monitor any vertical movement of the embankment and the berm using the LPs, thin plastic platforms (approximately 25mm × 25mm in plan at model scale) were placed on the sand surface directly below the LPs. To measure the horizontal movement of the embankment and the berm, the LPs' rod was attached to an aluminum flag in front of the LPs (Figure 6). The aluminum flags were fixed to the berm using four 20-mm nails.

2.3 Input motions

The model was shaken with a sequence of 4 shaking events consisting of one step motion, and three seismic motions of varying intensity. The seismic input motions were scaled versions of a motion derived from a downhole recording at Port Island during the 1995 Kobe earthquake (Wilson et al. 1997) with peak horizontal base accelerations in the range of 0.06, 0.26, and 0.54g.

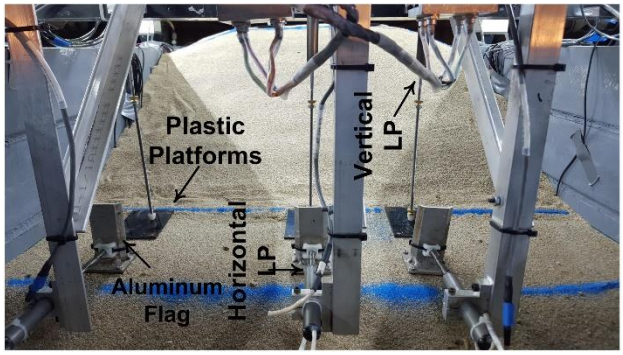

Figure 6. Configurations of LP system for vertical and horizontal displacement measurement of the embankment and the berm

3 DYNAMIC RESPONSES

The dynamic responses of the soil-cement wall system and supported embankment are presented together using select motions to illustrate the observed behaviors. Responses are presented for the medium- and high-intensity Kobe motions, whereas responses for all other motions can be found in the data report (Khosravi et al. 2016b).

3.1 Acceleration Time Histories

Acceleration responses of the soil foundation and embankment are shown in Figs. 7 and 8 for Kobe motion with peak base accelerations (PBA) of 0.26g and 0.54g, respectively. Each figure shows horizontal motions recorded in the soil between the walls and near the foundation surface (Soil-S14), on the wall under the berm (Wall-Berm), on the berm of the embankment (Berm-E06), on the crest (Crest-E18), in the soil under the embankment and near the foundation surface (Soil-S11) and the input base motion.

The acceleration responses of the soil foundation (Soil-S14) show strong high frequency acceleration spikes that are associated with the cyclic mobility behaviors. For the motion with PBA=0.26g (Figure 7), the peak horizontal acceleration (PHA) in the soil between the walls and near the foundation surface (Soil-S14) was 0.69g, while in the soil under the embankment and near the foundation surface (Soil-S11), a PHA of 0.23g was recorded. For the motion with PBA = 0.54g (Figure 8), PHAs in both S14 and S11 were approximately 0.69g. Results also indicated richer long-period components for the layer of loose sand, specifically in the stronger shaking event, which is an indication of liquefaction of the sand layer.

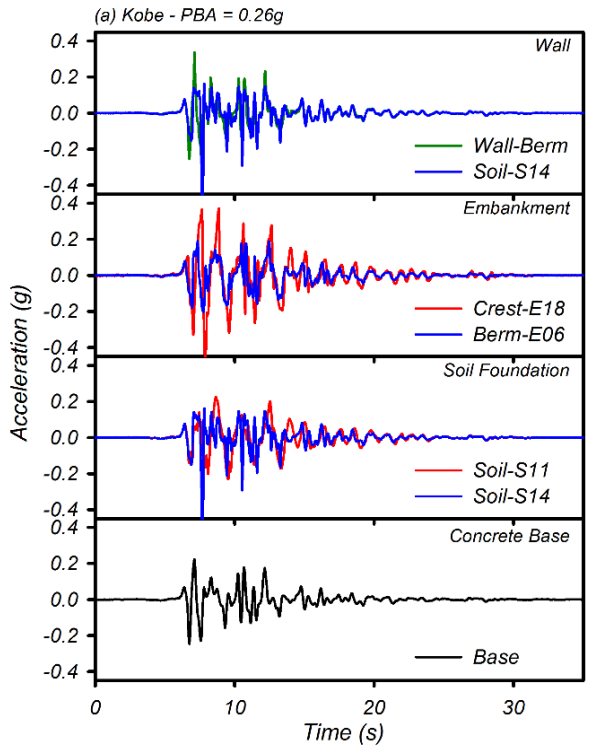

Figure 7. Recorded accelerations in the soil, embankment, and walls during Kobe Motion with PBA = 0.26g.

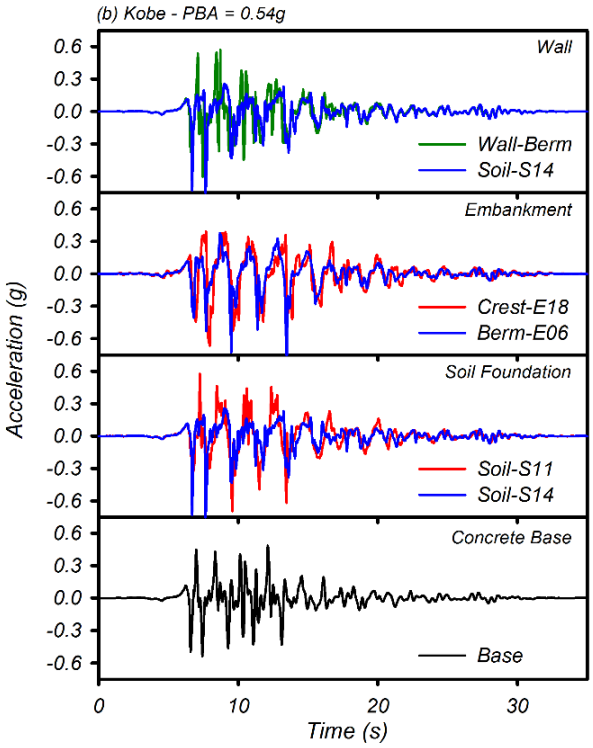

Figure 8. Recorded accelerations in the soil, embankment, and walls during Kobe Motion with PBA = 0.54g.

In the embankment, the PHAs were amplified up through the embankment, reaching values of 0.40g (Figure 7) and 0.60g (Figure 8) at the crest during the PBA=0.26 and 0.54g events, respectively. The acceleration responses also showed a peculiar asymmetric response, occurred with clear spikes during shaking, specifically during the PBA=0.54g event (Figure 8); a response which is attributed to the occurrence of seismic downslope deformation of the embankment. Similar observations were reported by other researchers such as Adalier et al. (1998). The walls showed acceleration responses very similar to the concrete base.

3.2 Pore Water Pressure Time Histories

The excess pore-water pressures (EPWP) measured for several points in the loose sand layer are shown in Figure 9 for the same Kobe motions with PBA = 0.26g (Figure 9a) and 0.54g (Figure 9b). Each figure shows EPWP in the soil underneath the embankment (P11), between the walls (Soil-P15), and at the toe (Soil-P16). Based on the results presented in Figure 9, the variations of EPWP in these two events were very similar in form. Their time-history responses could be divided into an initial build-up stage, a sustained level of high excess pore pressures during strong shaking, and a dissipation stage. In the build-up stage, the EPWPs responded in highly oscillatory fashion, which is attributed primarily to the soil skeleton's tendency to dilate at large strain (i.e. cyclic mobility behavior). During both medium- and high-intensity motions, initially the EPWP raised to values equal to the estimated overburden stresses at these points, indicating that excess pore water pressure ratios of, or near, 100% were triggered throughout the loose sand layer. In the dissipation stage, the EPWPs began dissipating after the strong shaking period of the motion (time ~20 s) with the dissipation being faster in the PBA=0.26g event. The measured excess pore water pressures were also observed to be far greater in soil under the embankment (P11) than in the free field beyond the toe (P16), reflecting the differences in overburden stresses at these points.

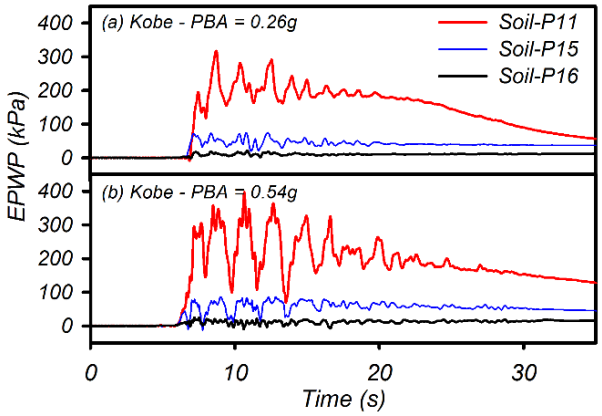

Figure 9. Excess pore water pressures in the liquefiable soil during Kobe motion with: a) PBA = 0.26g, and b) PBA = 0.54g

3.3 Embankment Response

Incremental shaking-induced vertical (settlement) of the embankment crest and berm for all shaking events are presented in Figure 10a and incremental horizontal displacement of the berm for all shaking events is presented in Figure 10b. The vertical displacement measurements indicated that the incremental crest settlement increased almost proportionately with the intensity of the shaking. The incremental shaking-induced settlement of the crest was about 320 mm for the motion with PBA=0.26g, while this value for the strongest motion with PBA=0.54g was about 640 mm. For the berm, the shaking-induced settlement was less than 50 mm for motions with PBA ≤ 0.26g and about 220 mm for the strongest motion with PBA=0.54g. The horizontal displacement of the berm over the treatment zone was about 320 mm and 1300 mm after shakings with PBA=0.26 and 0.54g, respectively.

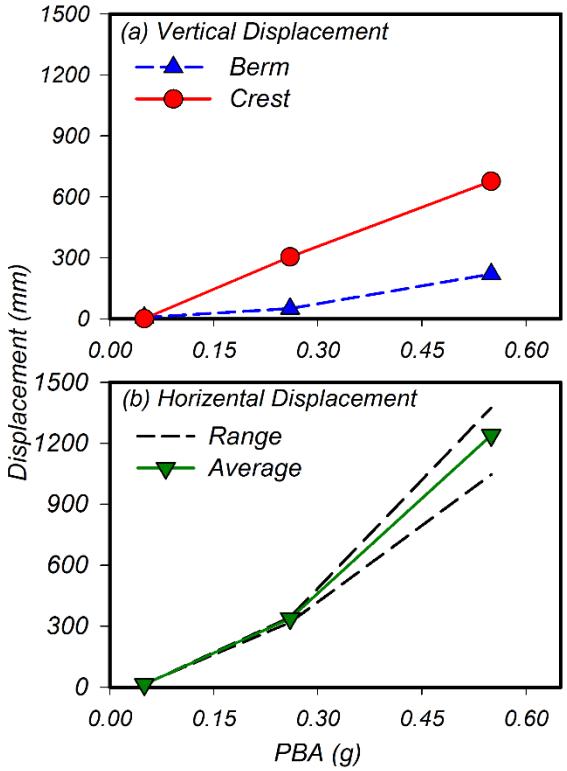

Figure 10. Incremental displacements of embankment during all shaking events: (a) vertical settlements of berm and crest, and (b) horizontal displacement of berm

The settlements of the embankment and berm are attributed to a combination of several contributing mechanisms, including shear deformation and cracking of the soil-cement walls, deformation of the liquefied loose sands through the spaces between the soil-cement walls, shear deformation of the embankment and loose sand layer outside the treatment zone, and post-liquefaction reconsolidation strains in the loose sand layer. Figure 11

presents contours of vertical settlement at the top of the loose sand layer based on mapping during post-testing excavation. These measurements show large settlements on the embankment side of the treatment zone (up to 600 mm), which are consistent with the combined influence of shearing deformation toward the toe and post-liquefaction reconsolidation strains in this area. These measurements also show heave (net upward movement) of the loose sand downstream of the treatment zone (up to 50 mm), which is attributed to the lateral movement of liquefied soil within the treatment zone causing a net lateral compression of the sand between the treatment zone and the container wall. This lateral compression causes upward vertical movement (or bulging) if the soil is largely undrained (no volume change), which is then offset by the post-liquefaction reconsolidation strains in this area. The photograph in Figure 12 shows damage patterns in the soil-cement walls as observed during post-testing excavation of the model. The cracking and offsets along the cracks are believed to have developed during the larger Kobe motion with PBS = 0.54 g, based on the crack detector measurements during shaking. In addition, examination of marker beds in the loose sand showed that the sand between the walls moved move than the walls in some locations and depths.

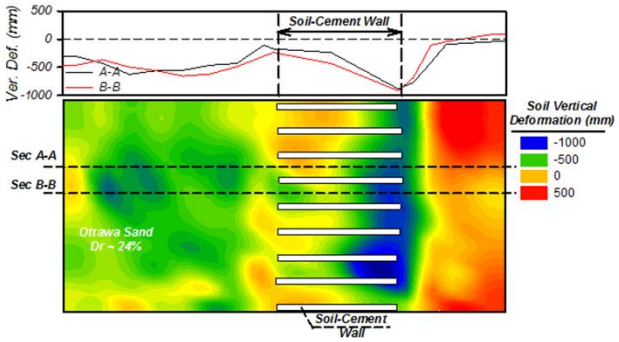

Figure 11- Contour of vertical displacement on Ottawa Sand after testing

Figure 12. Post-test excavation photo of the soil-cement walls (toe of berm is on left side of photograph)

4 CONCLUSION

The seismic performance of an embankment overlying a liquefiable soil layer which was treated with a series of soil-cement walls was investigated using the 9-m radius centrifuge at the Center for Geotechnical Modeling at UC Davis. Recorded responses during three shaking events of varying intensity were used to examine the seismic behavior of an embankment over treated soft soil and the shear response and performance of the soil-cement wall reinforcements under strong enough shaking to extensively damage the walls.

The observed responses included high frequency acceleration spikes attributed to cyclic mobility behavior in the liquefied sand layer, along with richer long-period components in the stronger shaking event. Peak accelerations were amplified up through the embankment, reaching their maximum values at the crest. The acceleration responses also showed an asymmetric response during shaking, which is attributed to the occurrence of seismic downslope deformation of the embankment. Excess pore water pressures in the loose sand equaled the estimated overburden stresses at different locations, and exhibited cyclic fluctuations consistent with cyclic mobility behaviors. The foundation soil's liquefaction contributed to the embankment vertical and horizontal displacements, with greater crest and berm displacements developing during shaking with greater intensity.

The experimental data have been archived for use by future researchers (Khosravi et al. 2016). The recorded responses provide a valuable dataset for evaluating design and analysis procedures for soil-cement wall reinforcement systems such as the two-dimensional nonlinear dynamic analyses methods presented by Boulanger et al. 2017 elsewhere in these proceedings.

5 ACKNOWLEDGMENTS

The centrifuge tests were supported by the State of California though the Pacific Earthquake Engineering Research Center (PEER). Any opinions, findings, or recommendations expressed herein are those of the authors and should not be interpreted as representing the official policies, either expressed or implied, of the above organizations. The assistance of the staff at the Center for Geotechnical Modeling is greatly appreciated.

6 REFERENCES

Adalier, K., Elgamal, A. K., and Martin, G. R. 1998. Foundation Liquefaction Countermeasures for Earth Embankments, *Journal of Geotechnical and Geoenvironmental Engineering*, ASCE, 124(6), 500-517.

Babasaki, R., Suzuki, K., Saitoh, S., Suzuki, Y., and Tokitoh, K. 1991. Construction and Testing of Deep Foundation Improvement Using the Deep Cement Mixing Method, *Deep Foundation Improvements: Design, Construction, and Testing*, ASTM STP 1089, Philadelphia, 224-234.

Boulanger, R. W., Khosravi, M., Khosravi, A., and Wilson, D. W. 2017. Remediation of liquefaction effects for an embankment using soil-cement walls: Centrifuge and numerical modeling. Proceedings, 3rd International Conference on Performance-based Design in Earthquake Geotechnical Engineering (PBD-III), Vancouver, Canada, July 16-29.

Kutter, B. L. 1995. Recent Advances in Centrifuge Modeling of Seismic Shaking (State-of-the-Art Paper), *Proceeding of 3rd International Conference on Recent Advances in Geotechnical Earthquake Engineering and Soil Dynamics*, 2, 927-942.

Khosravi, M., Tamura, S., Boulanger, R. W., Wilson, D. W., Olgun, C. G., Rayamajhi, D., Wang, Y. 2015a. Dynamic Centrifuge Tests on Soft Clay Reinforced by Soil-Cement Grids. IFCEE 2015, 2349-2358, doi 10.1061/9780784479087.218.

Khosravi, M., Boulanger, R. W., Wilson, D. W., Tamura, S., Olgun, C. G., Wang, Y., 2015b. Seismic Performance of Soil-Cement Grid Supporting a Structure over Soft Clay. The Deep Mixing 2015 Conference, San Francisco, CA, 631-640.

Khosravi, M., Boulanger, R., Tamura, S., Wilson, D., Olgun, C., and Wang, Y. 2016a. Dynamic Centrifuge Tests of Soft Clay Reinforced by Soil–Cement Grids. J. Geotech. Geoenviron. Eng., 10.1061/(ASCE)GT. 1943-5606.0001487, 04016027.

Khosravi, A., Khosravi, M., Pulido, A., Wilson, D. W., and Boulanger R. W. 2016b. Remediation of Liquefaction Effects for a Dam using Soil-Cement- Walls. Center for Geotechnical Modeling, Davis, CA.

Kitazume, M. and Karastanev, D. 1996. Bearing capacity of improved ground with column type DMM, Grouting and Deep Mixing, *Proceedings of IS-Tokyo 96*, 2nd International Conference on Ground Improvement Geosystems, 503-508.

Mitchell, J.K. 2008. Mitigation of Liquefaction Potential of Silty Sands, *From Research to Practice in Geotechnical Engineering Congress*, 433-451.

Rayamajhi, D., Tamura, S., Khosravi, M., Boulanger, R.W., Wilson, D., Ashford, S.A., and Olgun, C.G. 2015a. Dynamic Centrifuge Tests to Evaluate Reinforcing Mechanisms of Soil-Cement Columns in Liquefiable Sand, *Journal of Geotechnical and Geoenvironmental Engineering*, 140(3), 04015015-1.

Rayamajhi, D., Tamura, S., Khosravi, M., Boulanger, R. W., Wilson, D. W., Ashford, S. A., Olgun, C. G. 2015b. Investigating Reinforcing Effects of Soil-Cement Columns in Liquefiable Sand Using Dynamic Centrifuge Tests. *The Deep Mixing 2015 Conference*, San Francisco, CA, 375-384.

Tamura, S., Khosravi, M., Boulanger, R.W., Wilson, D. W., Olgun, C.G., Rayamajhi, D., Wang, Y. 2015. Seismic response of Soft Clay Reinforced by Soil-Cement Grid Based on Dynamic Centrifuge Tests. 6th International Conference on Earthquake Geotechnical Engineering, 1-4 November 2015, Christchurch, New Zealand.

Wilson, D. W., Boulanger, R. W., Kutter, B. L., and Abghari, A. (1997). 'Aspects of dynamic centrifuge testing of soil-pile-superstructure interaction.' Observation and modeling in numerical analysis and model tests in dynamic soil-structure interaction problems, Geotech. Spec. Publ. No. 64, T. Nogami, ed., ASCE, New York, 47–63.